

Electronic, elastic and optical properties on the $Zn_{1-x}Mg_xSe$ mixed alloys

G. Surucu · K. Colakoglu · E. Deligoz ·
Y. Ciftci · N. Korozlu

Received: 13 April 2010/Accepted: 23 August 2010/Published online: 8 September 2010
© Springer Science+Business Media, LLC 2010

Abstract The structural, elastic, electronic and optical properties of $Zn_{1-x}Mg_xSe$ ternary mixed crystals are investigated by utilizing the first-principles plane-wave pseudopotential method within the LDA approximations. Some basic physical properties, such as lattice constant, bulk modulus, second-order elastic constants (C_{ij}), Shear modulus, Young's modulus, Poisson's ratio, Lamé constants and the electronic band structures, are calculated. We have, also, predicted the optical properties such as dielectric functions, refractive index and energy loss function of these ternary mixed crystals. Our results agree well with the available data in the literature.

Introduction

There is a continuing interest in wide gap II–VI ternary and quaternary alloys for their optoelectronic applications [1–6]. These materials are used to fabricate X-ray and γ -ray detectors [2, 3]. Due to their direct and rather large gap character, ZnSe based semiconductors have been proposed a variety of new materials for optoelectronics. The usefulness of the $Zn_{1-x}Mg_xSe$ type of mixed crystals stems from the possibility of tuning of band gap energies and

lattice constants by adjusting the content of particular elements [4].

$Zn_{1-x}Mg_xSe$ have been studied experimentally and theoretically recently and in the past decades. Firszt et al [1, 7] have investigated photoluminescence characteristics as a function of temperature for $Zn_{1-x}Mg_xSe$ ($0 < x < 0.63$) grown by the high pressure Bridgman method. Derkowska et al [4–6] have studied experimentally the linear/non-linear optical properties of $Zn_{1-x}Mg_xSe$. Varshney et al [8] have analyzed the elastic properties and phase transition pressure in diluted magnetic semiconductors $Zn_{1-x}Mg_xSe$ ($x = 0.016, 0.026$ and 0.053) by using a three-body potential interactions. Benkabou et al [9] have studied the composition dependence of the positron annihilation in $Zn_{1-x}Mg_xSe$ by using the pseudopotential method.

As far as we know, there are no systematic theoretical studies on the structural elastic, electronic and optical properties of $Zn_{1-x}Mg_xSe$ mixed crystals in the concerning literature. An accurate description of these properties, as well as for guiding the successful design and fabrication of optoelectronic devices [10], plays a significant role in determining some material properties such as interatomic forces, phase transition, transport coefficients and electron–photon interactions.

In this work, we have aimed to provide some additional information to existing data on the physical properties of $Zn_{1-x}Mg_xSe$ mixed crystals by using the first-principles plane-wave pseudopotential method. Particularly, we focused on the composition-dependence of elastic and optical properties of $Zn_{1-x}Mg_xSe$. The layout of this paper is as follows: the method of calculation is given in ‘Method of calculation’ section. The results and overall conclusion are presented and discussed in ‘Results and discussion’ and ‘Summary and conclusion’ sections, respectively.

We have also presented the composition-dependence of elastic properties and our other results on the structural and

G. Surucu · K. Colakoglu · Y. Ciftci
Department of Physics, Gazi University, Teknikokullar,
06500 Ankara, Turkey

E. Deligoz (✉)
Department of Physics, Aksaray University,
68100 Aksaray, Turkey
e-mail: edeligoz@yahoo.com

N. Korozlu
Department of Physics, Erzincan University, Basbaglar,
24100 Erzincan, Turkey

elastic properties for $Zn_{1-x}Mg_xSe$ mixed crystals. The obtained results are compared with the previous theoretical calculations and available experimental findings.

Method of calculation

The calculations have been performed by using the plane-wave pseudopotential approach to the density-functional theory (DFT) by Cambridge Sequential Total Energy Package (CASTEP) code [11]. The electronic wave functions were obtained by using a density-mixing minimization method for the self-consistent field (SCF) calculation, and the structures were relaxed by using the Broyden, Fletcher, Goldfarb and Shannon (BFGS) method [12]. It solves the quantum mechanical equation for the electrons within density functional approach in the local-density approximation (LDA). For LDA, the exchange-correlation functional of Ceperley and Adler [13] as parameterized by Perdew and Zunger [14] was used.

The tolerances for geometry optimization were set as the difference in total energy being within 5×10^{-6} eV/atom, the maximum ionic Hellmann–Feynman force within 0.01 eV/Å, the maximum ionic displacement within 5×10^{-4} Å, and the maximum stress within 0.02 GPa. The interactions between electrons and core ions are simulated with separable Troullier–Martins [15] norm-conserving pseudopotentials. The wave functions are expanded in the plane waves up to a kinetic-energy cutoff of 660 eV. In this paper, the k -points of $6 \times 6 \times 4$ for $x = 0.5$ and $4 \times 4 \times 4$ for the other composition x , which are in the Monkhorst and Pack scheme, are used.

Results and discussion

Structural and electronic properties

The calculated most possible crystal structures and bond lengths for $Zn_{1-x}Mg_xSe$ are given in Table 1 and Fig. 1. The results for ZnSe and MgSe are completely compatible with the literature [16–19]. There is no other study except for the values of $x = 0$ and $x = 1$. Therefore, a comparison cannot be made for $x = 0.25, 0.50$ and 0.75 . When the composition x increases, the bond lengths increase due to the increasing of the cell volume.

Table 2 shows the calculated lattice constants, cell volumes and bulk modulus for each x of $Zn_{1-x}Mg_xSe$ along with the other experimental and theoretical values [9, 16, 17, 20–25]. The lattice parameters are found as 5.69, 5.75, 4.10, 5.87, 5.93 Å for $Zn_{1-x}Mg_xSe$ compounds ($x = 0, 0.25, 0.5, 0.75, 1$), respectively. The calculated lattice constants are higher (about 1%) for ZnSe compound than

Table 1 Bond length of $Zn_{1-x}Mg_xSe$

	Structure	Reference	Zn–Se (Å)	Se–Mg (Å)
ZnSe	Zinc-blende ($F\bar{4}3m$)	Present	2.466	
		Theory ^a	2.593	
		Theory ^b	2.463	
		Expt. ^c	2.454	
		Expt. ^d	2.454	
$Zn_{0.75}Mg_{0.25}Se$	Sylvanite ($P4\bar{3}m$)	Present	2.486	2.564
$Zn_{0.5}Mg_{0.5}Se$	Tetragonal ($P\bar{4}m2$)	Present	2.481	2.556
$Zn_{0.25}Mg_{0.75}Se$	Sylvanite ($P4\bar{3}m$)	Present	2.475	2.546
MgSe	Zinc-blende ($F\bar{4}3m$)	Present		2.569
		Theory ^a		2.473
		Theory ^b		2.543
		Expt. ^d		2.550

^a Reference [19]

^b Reference [17]

^c Reference [18]

^d Reference [16]

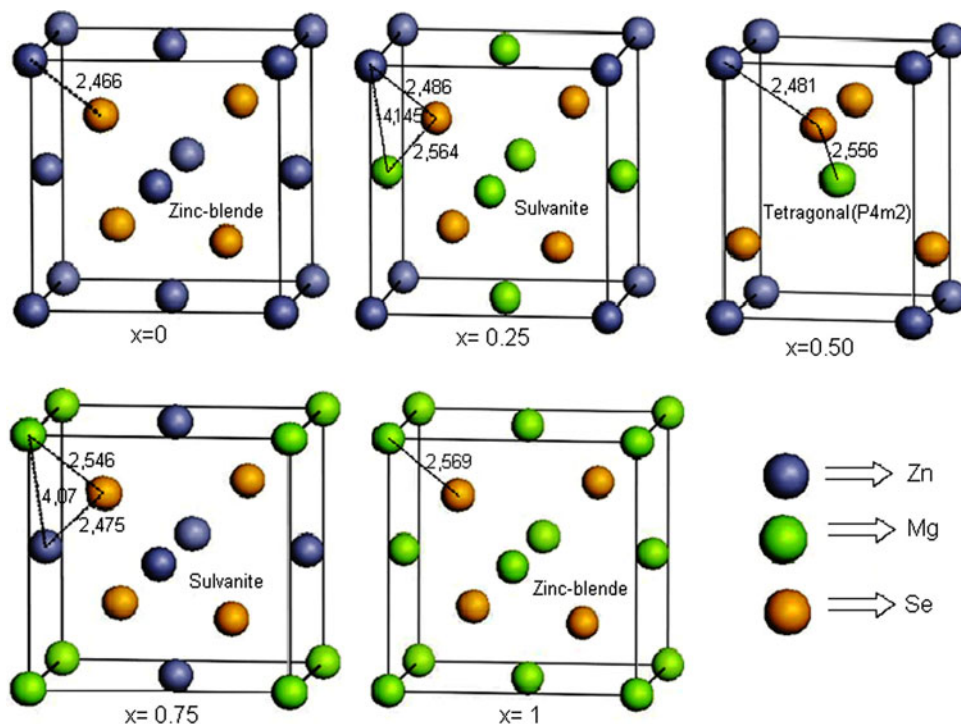
the other theoretical findings in [9, 17, 20, 24] and for MgSe compound than the other theoretical findings in [9, 17, 20–22] and smaller (about 1%) for ZnSe compound than theoretical finding in [24] and for MgSe compound than theoretical finding in [23, 25]. Our lattice constants are 1% higher for ZnSe and MgSe than the experimental value of [16, 22]. These small differences may come from different density functional based electronic structure method. The MgSe has the largest lattice constant (5.93 Å), and $Zn_{0.5}Mg_{0.5}Se$ has the smallest (4.4 Å) one for $Zn_{1-x}Mg_xSe$.

In the present case, the calculated bulk modulus for $x = 0, 0.25, 0.5, 0.75$ and 1 are 68.81, 61.84, 56.76, 52.64 and 49.47 GPa for $Zn_{1-x}Mg_xSe$, respectively. The bulk modulus versus composition x (0, 0.25, 0.5, 0.75, and 1) plot is shown in Fig. 2. To see the expected deviation from Vegard's law, for bulk modulus, we have used the following relation:

$$B(Zn_{1-x}Mg_xSe) = (1 - x)B^{ZnSe} + xB^{MgSe} - bx(1 - x) \quad (1)$$

where the quadratic term b represents the disordered parameter (bowing). It can be seen that the bulk modulus of these alloys decreases with the increasing of the composition x . The deviation from Vegard's law, which may also stem from the lattice mismatch between ZnSe and CaSe compounds, is found to be 16.34 GPa for these alloys. The calculated data suggest that the sequence of the compressibility from low to high is: ZnSe < $Zn_{0.75}Mg_{0.25}Se$ < $Zn_{0.5}Mg_{0.5}Se$ < $Zn_{0.25}Mg_{0.75}Se$ < MgSe. For these

Fig. 1 Crystal structures and bond length of $Zn_{1-x}Mg_xSe$ ($x = 0, 0.25, 0.5, 0.75, 1.0$)



configurations, the largest value of bulk modulus (65.86 GPa) obtained for ZnSe implies that it is a relatively less compressible compound.

We have predicted the band structures for $Zn_{1-x}Mg_xSe$ along the high symmetry directions in the first Brillouin zone from the calculated equilibrium lattice constant. Figure 3 shows the band structures and corresponding electronic density of state (DOS) for all compositions studied. All these materials have a direct band gap along the Γ direction, and the obtained results are listed in Table 3 with the some other theoretical and experimental values [16, 17, 21–23, 26, 27]. The band profiles and band gap values are in good agreement with the earlier theoretical works for ZnSe and MgSe. When we applied the empirical scissors operator, our results are consistent with the experimental values of [28]. When the x values ($x = 0, 0.25, 0.5, 0.75$) increased, the energy band gap increases as shown in Fig. 4. Also, the lowest valence bands occur at $-12.86, -12.46, -12.10, -11.70$ and -11.30 eV for $Zn_{1-x}Mg_xSe$ compounds ($x = 0, 0.25, 0.5, 0.75, 1$). The results show that the lowest value of valence band (-12.86 eV), corresponding to $x = 0$, belongs to ZnSe, and the other lowest one (-11.30 eV), corresponding to $x = 1$, belongs to MgSe. Namely, the value of the valence band width has similar trend with the energy band gap. The calculated energy-gap values, $E_g^{\Gamma-\Gamma}$, at different concentrations are fitted to do second-order polynomial equation

$$E_g^{\Gamma-\Gamma} = 1.33 + 0.76x + 0.55x^2 \quad (2)$$

as shown in Fig. 4. From this equation, one can easily reproduce the energy-gap value of the end point compounds ZnSe and CaSe. These calculated energy-gap values of the studied alloys are also compared with those obtained using empirical electronegativity expression

$$E_g^{Zn_{1-x}Mg_xSe} = (1 - x)E_g^{ZnSe} + xE_g^{MgSe} - \Delta\chi(1 - x) \quad (3)$$

where $\Delta\chi$ represents the electronegativity difference between Zn and Mg cations 1.65 and 1, respectively. The results of Eqs. 2, 3 are plotted as a function of composition x in Fig. 4. The results derived from the electronegativity considerations in Fig. 4, significantly, deviate from the fitted equation, probably due to the cations Zn and Mg belong to the different groups in the periodic table. Unfortunately, to compare with the present values, other theoretical or experimental data are not available yet, except the end-point compound ZnSe.

Elastic properties

The elastic constants of solids provide a link between the mechanical and dynamical behaviour of crystals, and give important information concerning the nature of the forces operating in solids. In particular, they provide information on the stability and stiffness of materials, and their ab initio calculation requires precise methods. Since the forces and

Table 2 Lattice constants, cell volume, bulk modulus of $\text{Zn}_{1-x}\text{Mg}_x\text{Se}$

	Structure	Reference	a_0 (Å)	b_0 (Å)	c_0 (Å)	V (Å ³)	B (GPa)
ZnSe	Zinc-blende ($F\bar{4}3m$)	Present	5.69			184.70	65.86
		Theory ^a	5.61				75.20
		Theory ^b	5.67				
		Theory ^c	5.74				56.80
		Theory ^d	5.68				63.90
		Theory ^e	5.62				71.82
		Expt. ^f	5.66				
		Expt. ^g	5.66				
$\text{Zn}_{0.75}\text{Mg}_{0.25}\text{Se}$	Sulvanite ($P4\bar{3}m$)	Present	5.75			190.65	61.84
$\text{Zn}_{0.5}\text{Mg}_{0.5}\text{Se}$	Tetragonal ($P\bar{4}m2$)	Present	4.10	4.10	5.84	98.27	56.76
$\text{Zn}_{0.25}\text{Mg}_{0.75}\text{Se}$	Sulvanite ($P4\bar{3}m$)	Present	5.87			202.78	52.64
MgSe	Zinc-blende ($F\bar{4}3m$)	Present	5.93			208.89	49.47
		Theory ^a	5.89				55.20
		Theory ^b	5.89				
		Theory ^c	6.00				45.10
		Theory ^d	5.87				47.00
		Theory ^h	5.97				47.80
		Theory ⁱ	5.92				49.00
		Expt. ^f	5.89				
		Expt. ^g	5.89				

^a Reference [20]

^b Reference [9]

^c Reference [23]

^d Reference [17]

^e Reference [24]

^f Reference [22]

^g Reference [16]

^h Reference [25]

ⁱ Reference [21]

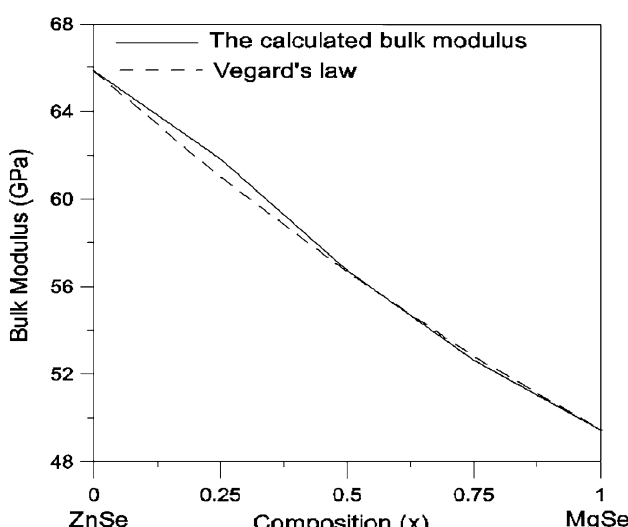


Fig. 2 Bulk modulus of $\text{Zn}_{1-x}\text{Mg}_x\text{Se}$ versus composition x

the elastic constants are functions of the first-order and second-order derivatives of the potentials, their calculation will provide a further check on the accuracy of the calculation of forces in solids. The second-order elastic constants (C_{ij}) are calculated by using the ‘volume-conserving’ technique [29, 30] and the results are given in Table 4.

For a stable tetragonal structure, the six independent elastic constants C_{ij} (C_{11} , C_{12} , C_{13} , C_{33} , C_{44} and C_{66}) should satisfy the well known Born–Huang criteria for stability [36] $C_{11} > 0$, $C_{33} > 0$, $C_{44} > 0$, $C_{66} > 0$, $(C_{11} - C_{12}) > 0$, $(C_{11} + C_{33} - 2C_{13}) > 0$, $[2(C_{11} + C_{12}) +$

$C_{33} + 4C_{13}] > 0$ while for cubic crystals, the three independent elastic constants C_{ij} (C_{11} , C_{12} , C_{44}) satisfy inequalities, $(C_{11} - C_{12}) > 0$, $C_{11} > 0$, $C_{44} > 0$, $(C_{11} + 2C_{12}) > 0$ [37].

Our results for elastic constants in Table 4 obey these stability conditions for each composition for considered $\text{Zn}_{1-x}\text{Mg}_x\text{Se}$ compounds.

In Fig. 5, the elastic constants, C_{11} , C_{12} , C_{44} , are shown, corresponding the x values. It can be seen that elastic constants of these alloys decrease, almost linear, with increase of the composition x . The values of C_{13} , C_{33} and C_{66} are only available for $\text{Zn}_{0.5}\text{Mg}_{0.5}\text{Se}$, and they are not shown in Fig. 5.

Shear modulus (G), Poisson’s ratio (ν), Young’s modulus (E) and Lamé constants (λ , μ), which are the most interesting elastic properties for applications, are often measured for polycrystalline materials when investigating their hardness. In Table 5, we list the calculated Shear modulus, Poisson’s ratio, Young’s modulus and Lamé constants along with the other theoretical values. These quantities are calculated based on the relations given in [38].

The $\nu = 0.25$ and 0.5 are the lower limit and upper limit for central force solids, respectively [39]. Our ν value is about 0.40 which indicates that the interatomic forces in the $\text{Zn}_{1-x}\text{Mg}_x\text{Se}$ are predominantly central forces. It is seen from Table 5 that while the calculated Shear modulus and Young’s modulus decrease on going from higher to lower composition x , the Poisson’s ratio increases. The calculated Young’s modulus for ZnSe is higher than that for the other

Fig. 3 Calculated band structures and DOS of $Zn_{1-x}Mg_xSe$ versus composition x . The position of the Fermi level (EF) is at 0 eV

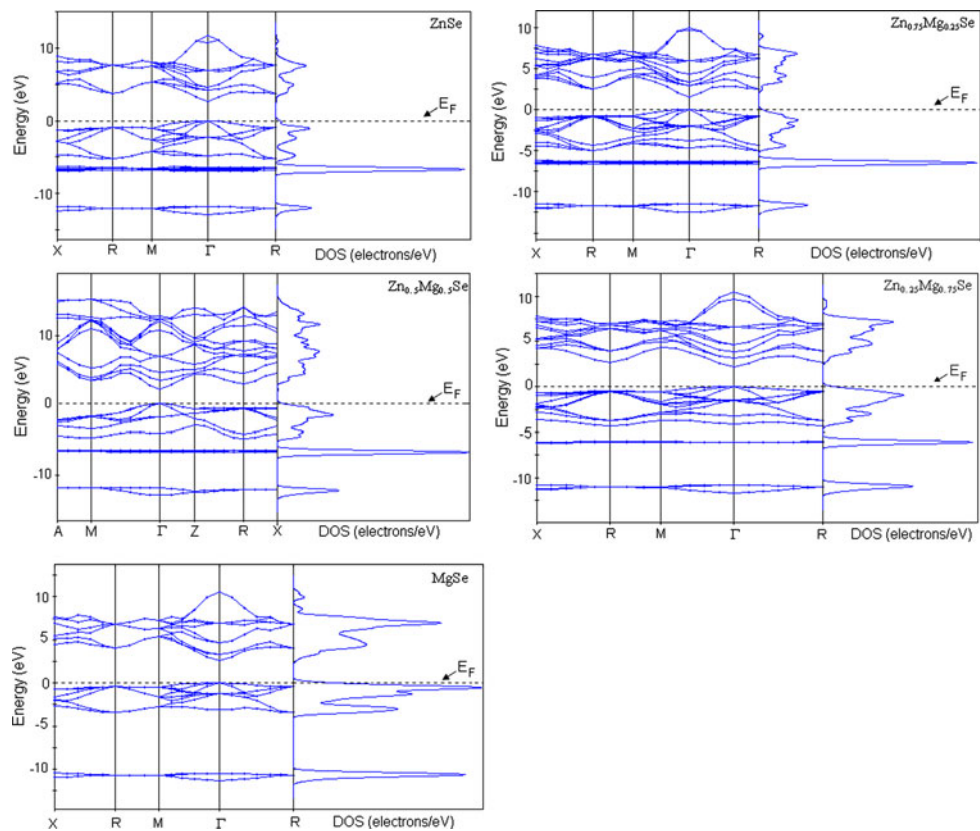


Table 3 The calculated energy band gaps of $Zn_{1-x}Mg_xSe$

	Structure	Reference	E_g (eV)
ZnSe	Zinc-blende ($F\bar{4}3m$)	Present	1.33
	Theory ^a		1.11
	Theory ^b		1.79
	Theory ^c		2.38
	Expt. ^d		2.72
	Expt. ^f		2.69
$Zn_{0.75}Mg_{0.25}Se$	Sulvanite ($P4\bar{3}m$)	Present	1.57
$Zn_{0.5}Mg_{0.5}Se$	Tetragonal ($P\bar{4}m2$)	Present	1.87
$Zn_{0.25}Mg_{0.75}Se$	Sulvanite ($P4\bar{3}m$)	Present	2.19
MgSe	Zinc-blende ($F\bar{4}3m$)	Present	2.66
$Zn_{1-x}Mg_xSe$	Theory ^a		2.49
	Theory ^b		2.81
	Theory ^c		2.82
	Theory ^d		2.40
	Theory ^e		2.47
	Expt. ^f		3.59
	Expt. ^g		3.59

^a Reference [23]

^b Reference [17]

^c Reference [27]

^d Reference [21]

^e Reference [26]

^f Reference [16]

^g Reference [22]

compounds with Mg. So, it is more stiffer alloy according to other ones.

According to criterion in Ref [40], a material is brittle (ductility) if the B/G ratio is less (high) than 1.75. In the present case, the value of the B/G is higher than 1.75 for the studied alloys, and hence, the present alloys will behave in a ductility manner.

Optical properties

To study the optical behaviour of $Zn_{1-x}Mg_xSe$, we use the dielectric function $\varepsilon(\omega)$ to describe the linear response of the system to electromagnetic radiation, which relates to the interaction of photons with electrons [41]. The real ($\varepsilon_1(\omega)$) and imaginary part ($\varepsilon_2(\omega)$) of the dielectric

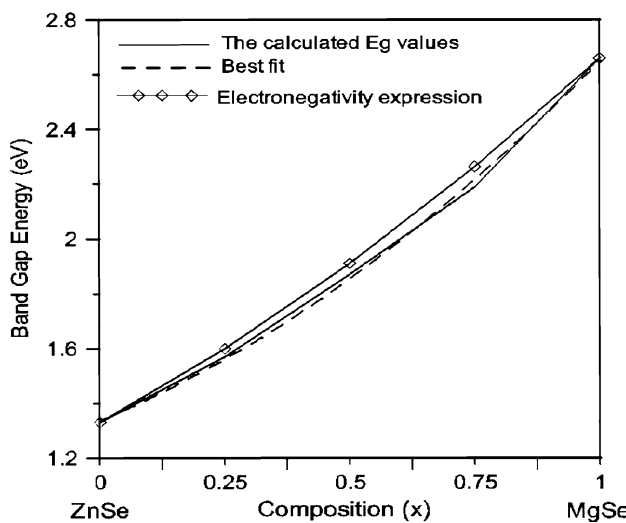


Fig. 4 Band gap energies of $Zn_{1-x}Mg_xSe$ versus composition x

functions are calculated as in our recent works [42–44] by using the usual Kramers–Kronig relationship in Ref [45]. These functions are displayed in Fig. 6 in the range of 0–24 eV, where the blue lines and red lines represent the real part $\varepsilon_1(\omega)$ and imaginary part $\varepsilon_2(\omega)$, respectively. The same peaks reduce due to the interband transition and approach to the minimum at about 6 eV for each composition x . For each composition x (0, 0.25, 0.50, 0.75, 1.0) of $Zn_{1-x}Mg_xSe$, dielectric constant, $\varepsilon_1(0)$, are found to be 6.50, 5.91, 5.59, 4.87, 4.38. For the imaginary part of the dielectric function for the same $Zn_{1-x}Mg_xSe$, the absorption starts at about 1.33, 1.57, 1.87, 2.19, 2.66 eV, respectively. The prominent peaks occur at about 6.37, 6.68, 6.98, 6.91, 6.94 eV for $Zn_{1-x}Mg_xSe$, respectively. Our peak

The main peaks of the real part of $Zn_{1-x}Mg_xSe$ arise at 3.71, 3.78, 3.82, 4.43, 4.88 eV respectively. The same peaks reduce due to the interband transition and approach to the minimum at about 6 eV for each composition x . For each composition x (0, 0.25, 0.50, 0.75, 1.0) of $Zn_{1-x}Mg_xSe$, dielectric constant, $\varepsilon_1(0)$, are found to be 6.50, 5.91, 5.59, 4.87, 4.38. For the imaginary part of the dielectric function for the same $Zn_{1-x}Mg_xSe$, the absorption starts at about 1.33, 1.57, 1.87, 2.19, 2.66 eV, respectively. The prominent peaks occur at about 6.37, 6.68, 6.98, 6.91, 6.94 eV for $Zn_{1-x}Mg_xSe$, respectively. Our peak

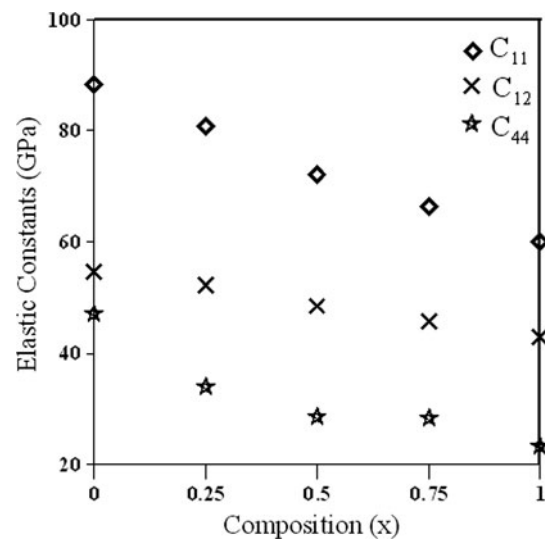


Fig. 5 Elastic constant of $Zn_{1-x}Mg_xSe$ versus composition x

values are consistent with the values of Refs. [27, 46] for $ZnSe$ and $MgSe$.

The dispersion curves of refractive index are plotted in Fig. 7 for each composition x ; and the refractive indices, $n(0)$, for $Zn_{1-x}Mg_xSe$ are found as 2.54, 2.42, 2.35, 2.20 and 2.09, respectively. The extinction coefficient, $(k(w))$, for each x are estimated as 1.46, 1.41, 1.78, 2.25, 2.45, respectively.

Finally, from the real and imaginary parts of the complex dielectric response function, the electron energy-loss function can be easily obtained. It is the imaginary part of the reciprocal of the complex dielectric function, and our results are displayed in Fig. 8. This function has a main peak so-called Plasmon frequency for each composition x at 15.96, 15.50, 17.66, 14.53, 13.96 eV, respectively. The composition-dependence of the Plasmon frequency does

Table 4 The calculated elastic constants (in GPa) $Zn_{1-x}Mg_xSe$

	Structure	Reference	C_{11}	C_{12}	C_{13}	C_{33}	C_{44}	C_{66}
$ZnSe$	Zinc-blende ($F\bar{4}3m$)	Present	88.33	54.62			47.21	
		Theory ^a	81.00	48.88			44.10	
		Theory ^b	85.90	44.20			41.90	
		Theory ^c	94.00	61.00			64.00	
		Theory ^d	85.20	51.70			–	
$Zn_{0.75}Mg_{0.25}Se$	Sulvanite ($P4\bar{3}m$)	Present	80.92	52.30			34.07	
$Zn_{0.5}Mg_{0.5}Se$	Tetragonal ($P\bar{4}m2$)	Present	72.16	48.53	49.36	71.98	28.57	28.42
$Zn_{0.25}Mg_{0.75}Se$	Sulvanite ($P4\bar{3}m$)	Present	66.39	45.76			28.40	
$MgSe$	Zinc-blende ($F\bar{4}3m$)	Present	60.00	42.84			23.22	
		Theory ^e	118.00	42.00			56.40	
		Theory ^f	63.22	43.86			44.76	
		Theory ^g	56.00	44.20			5.59	
		Theory ^g	63.10	61.80			6.92	
		Theory ^h	56.30	48.70			–	

^a Reference [31]

^b Reference [34]

^c Reference [24]

^d Reference [16]

^e Reference [33]

^f Reference [27]

^g Reference [32]

^h Reference [35]

Table 5 The calculated Poisson's ratio (ν), Young's modulus (E), Shear modulus (G), Lamé constants (λ, μ) for $Zn_{1-x}Mg_xSe$

	Structure	Reference	G (GPa)	E (GPa)	ν	λ (GPa)	μ (GPa)
ZnSe	Zinc-blende ($F\bar{4}3m$)	Present	31.25	46.58	0.38	6.08	47.21
		Theory ^a	28.90	75.70	—	—	—
$Zn_{0.75}Mg_{0.25}Se$	Sulvanite ($P4\bar{3}m$)	Present	24.05	39.85	0.39	12.77	34.07
$Zn_{0.5}Mg_{0.5}Se$	Tetragonal ($P\bar{4}2m$)	Present	21.66	32.67	0.38	15.06	28.52
$Zn_{0.25}Mg_{0.75}Se$	Sulvanite ($P4\bar{3}m$)	Present	18.93	29.04	0.41	9.58	28.40
MgSe	Zinc-blende ($F\bar{4}3m$)	Present	15.58	24.31	0.41	13.55	23.22

^a Reference [41]

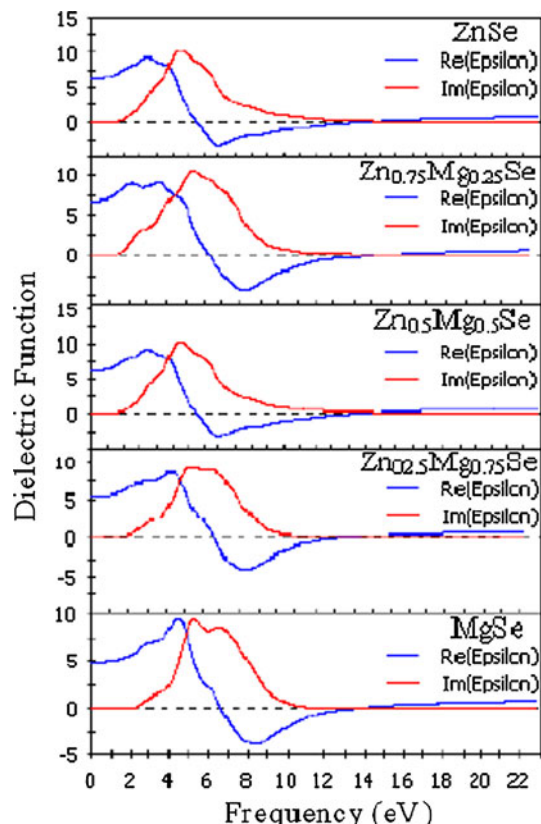


Fig. 6 The real and imaginary part of dielectric function (Color figure online)

not show a regular changing. However, it is seen that the highest-value is found for $x = 0.5$ ($P\bar{4}2m$ structure) of $Zn_{1-x}Mg_xSe$ compounds.

Summary and conclusion

In this work, we have presented structural, elastic, electronic and optical properties of the $Zn_{1-x}Mg_xSe$ ternary mixed crystals by using the first principles calculations based on the plane-wave pseudopotential method within the LDA approximation. Specifically, the lattice constants,

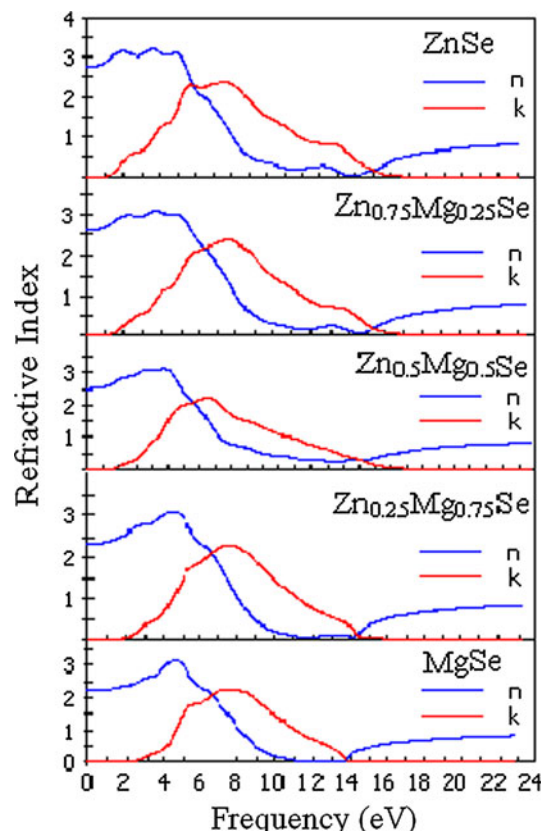


Fig. 7 Refractive index, n , and extinction coefficient, k

bulk modulus, the pressure derivative of bulk modulus, energy band gap, zero-pressure elastic constants and their related quantities, such as Young's modulus, Shear modulus, Poisson's ratio and Lamé constants are calculated. The MgSe has the largest lattice constant (5.93 Å), and $Zn_{0.5}Mg_{0.5}Se$ has the smallest (4.10 Å) one for $Zn_{1-x}Mg_xSe$. The bond distances and the cell volumes show similar trend for same compositions. ZnSe has the lowest compressibility and it may be a less compressible compound. The composition dependence of the lattice constant and bulk modulus are found almost, to be linear. The elastic constants satisfy the traditional mechanical stability conditions for all considered structures. For all

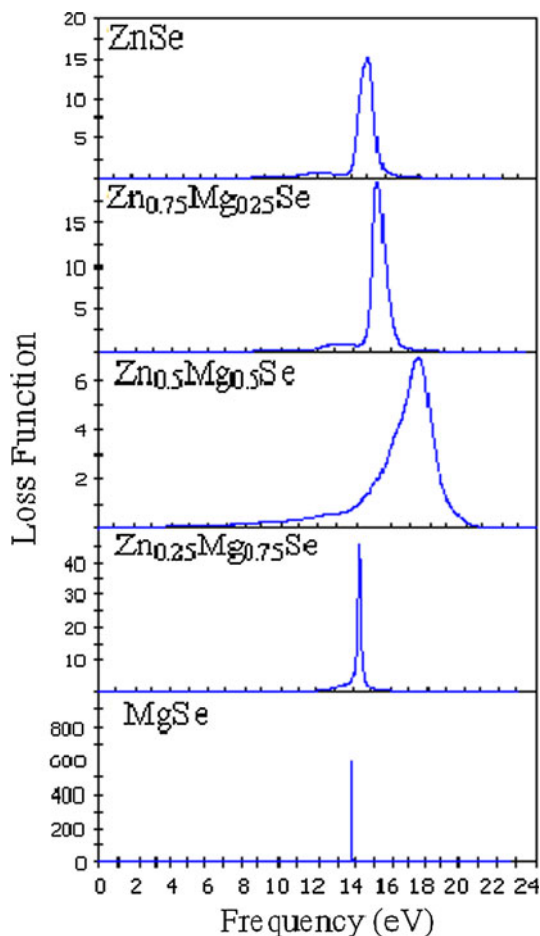


Fig. 8 Loss function $L(\omega)$

compositions (x) these compounds are characterized as a direct band gap material along the Γ direction. The considered optical properties are consistent with the available experimental and the theoretical findings.

Acknowledgements This work is supported by Gazi University Research-Project Unit under Project No: 05/2008-42.

References

1. Firszt F, Meczynska H, Legowski S, Paszkowicz W (2004) *J Alloys Compd* 371:107
2. Eisen Y, Shor A (1998) *J Cryst Growth* 184–185:1302
3. Hannachi L, Bouarissa N (2008) *Superlattices Microstruct* 44:794
4. Derkowska B, Essaidi Z, Sahraoui B, Marasek A, Firszt F, Kujawa M (2009) *Opt Mater* 31:518
5. Derkowska B, Firszt F, Sahraoui B, Marasek A, Kujawa M (2008) *Opto-electronics Rev* 16:8
6. Derkowska B, Wojdyla M, Plociennik P, Sahraoui B, Bala W (2004) *Opto-electronics Rev* 12:405
7. Firszt F, Legowski S, Meczynska H, Huang CT, Hsu HP, Huang YS (2008) *J Korean Phys Soc* 53:13
8. Varshney D, Sharma P, Kaurav N, Shah S, Singh RK (2005) *J Phys Soc Jpn* 74:382
9. Benkaboua F, Aouraga H, Certierb M, Kobayasic T (2003) *Physica B* 336:275
10. Polit JJ, Sheregi EM, Burattini E, Marcelli A, Cestelli Guidi M, Calvani P, Nucara A, Piccinini M, Kisiel A, Konior J, Sciesinska E, Sciesinski J, Mycielski A (2004) *J Alloy Compd* 371:172
11. Segall MD, Lindan PJD, Probert MJ, Pickard CJ, Hasnip PJ, Clark SJ, Payne MC (2002) *J Phys Condens Mater* 14:2717
12. Zhu W, Xiao H, Comput J (2008) *J Comput Chem* 29:176
13. Ceperley DM, Alder BJ (1980) *J Phys Rev Lett* 45:566
14. Perdew JP, Zunger A (1981) *Phys Rev B* 23:5048
15. Troullier N, Martins JL (1991) *Phys Rev B* 43:1993
16. Hernández Calderón I (2002) Semiconductor materials and their applications, vol 12. Taylor and Francis, New York, p 113
17. Lee S-G, Chang KJ (1995) *J Phys Rev B* 52:1918
18. Vérité C (1997) *Mater Sci Eng B* 43:60
19. Reddy RR, Nazeer Aharnmed Y, Abdul Azeem P, Rama Gopal K, Sasikala Devi B, Rao TVR (2003) *Def Sci J* 53:239
20. Rabah M, Abbar B, Al-Douri Y, Bouhafs B, Sahraoui B (2003) *Mater Sci Eng B* 100:163
21. Duman S, Bağcı S, Tütüncü HM, Srivastava GP (2006) *Phys Rev B* 73:205201
22. Okuyama H, Kishita Y, Ishibashi A (1998) *Phys Rev B* 57:2257
23. El Haj Hassan F, Javad Hashemifar S, Akbarzadeh H (2006) *Phys Rev B* 73:195202
24. Khenata R, Bouhemadou A, Sahnoun M, Reshak Ali H, Baltache H, Rabah M (2006) *Comput Mater Sci* 38:29
25. Van Camp PE, Van Doren VE (1997) *Phys Rev B* 55:775
26. Fleszar A (2001) *Phys Rev B* 64:245204
27. Drief F, Tadjer A, Mesri D, Aourag H (2004) *Catal Today* 89:343
28. Clark SJ, Segall MD, Pickard CJ, Hasnip PJ, Matt I, Probert J, Refson K, Payne MC (2005) *Z Kristallogr* 220:567
29. Ashcroft NW, Mermin ND (1976) Solid state physics. Saunders College, Philadelphia
30. Nye JF (1957) Physical properties of crystals. Clarendon, Oxford
31. Martin RM (1970) *Phys Rev B* 1:4005
32. Rached D, Benkhettou N, Soudini B, Abbar B, Sekkal N, Driz M (2003) *Phys Stat Sol B* 240:565
33. Marinelli F, Dupin H, Lichanot A (2000) *J Phys Chem Solids* 61:1707
34. Anil TV, Menon CS, Kumar SK, Jayachandran KP (2004) *J Phys Chem Solids* 65:1053
35. Chung TY, Ohz JH, Lee SG, Jeong JW, Chang KJ (1997) *Semicond Sci Technol* 12:701
36. Born M, Huang K (1956) Dynamical theory of crystal lattices. Clarendon, Oxford
37. Shein IR, Ivanovskii AL (2008) *Physica C* 468:2224
38. Kitamura M, Muramatsu S, Harrison WA (1992) *Phys Rev B* 46:1351
39. Fu H, Li D, Peng F, Gao T, Cheng X (2008) *Comput Mater Sci* 44:774
40. Shein IR, Ivanovskii AL (2008) *J Phys Condens Matter* 20:415218
41. Sun J, Wang HT, Ming NB (2004) *Appl Phys Lett* 84:4544
42. Surucu G, Colakoglu K, Deligoz E, Korozlu N, Ciftci YO (2010) *Solid State Commun* 150:1413
43. Korozlu N, Colakoglu K, Deligoz E (2009) *J Phys Condens Matter* 21:175406
44. Korozlu N, Colakoglu K, Deligoz E (2010) *Phys Status Solidi B* 247:1214
45. Hu JM, Huang SP, Xie Z, Hu H, Cheng WD (2007) *J Phys Condens Matter* 19:496215
46. Adachi S, Taguchi T (1991) *Phys Rev B* 43:9569